

# Orthogonal Low-rank Adaptation in Lie Groups for Continual Learning of Large Language Models

Kefan Cao and Shuaicheng Wu

Yingcai Honor College,  
University of Electronic Science and Technology of China

## Abstract

Large language models (LLMs) are prone to catastrophic forgetting in sequential multi-task settings. Parameter regularization methods such as O-LoRA and N-LoRA alleviate task interference by enforcing low-rank subspace orthogonality, but they overlook the fact that conventional additive fine-tuning disrupts the intrinsic geometric structure of LLM parameters, limiting performance. Our key insight is that the parameter space of LLMs possesses a geometric structure, which must be preserved in addition to enforcing orthogonality. Based on this, we propose Orthogonal Low-rank Adaptation in Lie Groups (**OLieRA**), which introduces Lie group theory into LLM fine-tuning: leveraging multiplicative updates to preserve parameter geometry while applying orthogonality constraints to task subspaces. Experiments demonstrate that OLieRA achieves state-of-the-art results on the Standard CL benchmark and remains among the top-performing methods in the Large Number of Tasks setting. Moreover, OLieRA inherits the core advantages of O-LoRA—no need for replay data and task-ID-free inference—establishing a new paradigm for continual learning in LLMs.

## 1 Introduction

Enabling lifelong continual learning in large language models (LLMs) is crucial for practical AI, yet they are prone to catastrophic forgetting across sequential tasks. To address the catastrophic forgetting issue (McCloskey and Cohen, 1989) faced by large language models (LLMs) in sequential multi-task scenarios, the research community has proposed continual learning as a solution—aiming to incrementally accumulate knowledge in non-stationary task streams while preventing the degradation of performance on previously learned tasks.

Existing continual learning approaches can be broadly categorized into three classes, each with notable limitations: (1)Replay-based methods

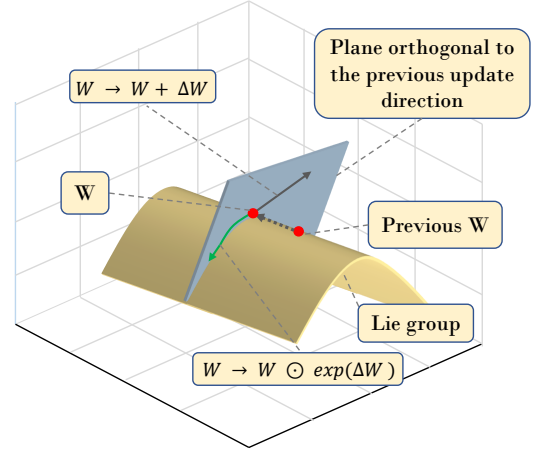


Figure 1: Illustration of the update mechanisms of OLieRA and O-LoRA. While O-LoRA updates parameters orthogonally to previously updated dimensions, it overlooks the intrinsic parameter structure. In contrast, OLieRA incorporates a Lie group constraint in addition to orthogonality, thereby preserving the original parameter structure.

(de Masson d’Autume et al., 2019): These methods store historical task data in a memory buffer and allow the model to revisit these samples during new task training. However, they require continuous storage of potentially sensitive user data, raising privacy concerns. Additionally, updating all model parameters leads to high computational costs. (2)Regularization-based methods (Kirkpatrick et al., 2017): These approaches introduce an additional regularization term in the loss function to penalize significant changes to important weights, thereby preserving knowledge from previous tasks. Nevertheless, most methods in this category suffer from degraded generalization in long task sequences and struggle to adapt to continuous multi-task learning settings. (3)Architecture-based methods (Razdaibiedina et al., 2023): These techniques dynamically expand model capacity or isolate task-specific parameters to minimize interfer-

ence. However, they essentially construct separate sub-models for different tasks, limiting their generalization to unseen tasks and reducing flexibility and universality.

Our work falls within the regularization-based paradigm and builds upon Orthogonal Low-Rank Adaptation (O-LoRA) (Wang et al., 2023a). Instead of updating parameters across a shared vector space for all tasks, O-LoRA performs gradient updates in directions orthogonal to the subspaces of previous tasks. This strategy has been shown to effectively mitigate catastrophic forgetting by avoiding interference with the loss landscapes of historical tasks.

In this paper, we propose Orthogonal Low-Rank Adaptation under Lie Groups (OLieRA). Unlike O-LoRA, which maintains orthogonality only within a specific low-rank subspace, OLieRA enforces orthogonality constraints directly across entire task subspaces. Moreover, it leverages Lie group theory to handle task subspaces. Compared to O-LoRA, OLieRA introduces only minimal additional computational overhead while achieving improved performance and enhanced theoretical interpretability. Figure 1 illustrates the conceptual differences between the update mechanisms of OLieRA and O-LoRA.

Thus, OLieRA retains all three key advantages of O-LoRA:

- a. *Data Privacy-Friendly*: Eliminates the need to store user data for replay, thereby resolving data privacy concerns at the source;
- b. *Parameter-Efficient*: Introduces only a small number of additional parameters, enabling efficient learning of new tasks without compromising performance on previous ones;
- c. *Generalization-Friendly*: Does not require task identity during testing, naturally aligns with instruction tuning paradigms, and effectively preserves the generalization ability of LLMs to unseen tasks.

Furthermore, OLieRA achieves comprehensive performance improvements, surpassing all existing methods in the orthogonal low-rank adaptation direction.

The core contributions of this study are as follows:

1. We propose OLieRA, a parameter regularization-based continual learning

framework grounded in Lie group theory. It significantly outperforms existing regularization-based methods such as O-LoRA and N-LoRA, achieving state-of-the-art (SOTA) results on the Standard CL Benchmark;

2. We apply Lie group theory to the fine-tuning process of LLMs, providing a geometric perspective for parameter updates that better preserves the intrinsic structure of the model’s representation space. Extensive analytical experiments validate the effectiveness and theoretical soundness of the proposed approach.

## 2 Related Work

### 2.1 Overview of Continual Learning

Continual Learning (Ke and Liu, 2023; Wang et al., 2023b) aims to develop learning algorithms that accumulate knowledge from non-stationary data streams. In supervised continual learning, a sequence of tasks  $\{\mathcal{D}_1, \dots, \mathcal{D}_T\}$  arrives sequentially. Each task  $\mathcal{D}_t = \{(x_i^t, y_i^t)\}_{i=1}^{n_t}$  contains an independent target dataset, where  $x_i^t \in \mathcal{X}_t$  and  $y_i^t \in \mathcal{Y}_t$ . A single model must adapt to these tasks incrementally, and at the  $t$ -th task, it can only access  $\mathcal{D}_t$ . Typically, given a predictive model  $h_\Theta$  parameterized by  $\Theta$ , the objective of continual learning is to optimize the following across all tasks:

$$\max_{\Theta} \sum_{k=1}^T \sum_{(x,y) \in \mathcal{D}_k} \log p_{\Theta}(y | x) \quad (1)$$

where  $p_{\Theta}(y|x)$  denotes the probability of predicting output  $y$  given input  $x$  under model  $h_{\Theta}$ .

### 2.2 LoRA

When adapting pre-trained models (PTMs) to specific tasks, it has been shown (Hu et al., 2021) that weight updates exhibit a low "intrinsic dimension." For a pre-trained weight matrix  $W \in \mathbb{R}^{d \times k}$ , LoRA constrains updates via low-rank decomposition:  $W + \Delta W = W + BA$ , where  $B \in \mathbb{R}^{d \times r}$ ,  $A \in \mathbb{R}^{r \times k}$ , and the rank satisfies  $r \ll \min(d, k)$ . During training,  $W$  remains fixed and does not receive gradient updates, while  $A$  and  $B$  contain trainable parameters. The modified forward pass for the computation  $h = Wx$  under LoRA becomes:

$$h = Wx + \Delta Wx = Wx + BAx$$

### 2.3 O-LoRA

O-LoRA (Wang et al., 2023a) is a framework for continual learning in language models. It first integrates human expertise and enhances generalization through instruction tuning. Then, for each incoming task, it incrementally learns a new LoRA module while enforcing orthogonality between the current task’s LoRA parameters and those of previous tasks.

We further elaborate on the notion of orthogonality in O-LoRA: Orthogonality in O-LoRA is enforced between the low-rank subspaces spanned by the LoRA parameters of different tasks.

Specifically, for each task  $t$ , the model learns a set of LoRA parameters  $\{A_t, B_t\}$ , where  $B_t \in \mathbb{R}^{d \times r_t}$  ( $d$  is the model dimension,  $r_t$  is the low rank). The parameter update subspace  $\mathcal{U}_t$  for task  $t$  is approximated as the span of the column vectors of  $B_t$ :

$$\mathcal{U}_t = \text{span}\{\mathbf{b}_t^1, \mathbf{b}_t^2, \dots, \mathbf{b}_t^{r_t}\} \quad (2)$$

where  $\mathbf{b}_t^i$  denotes the  $i$ -th column vector of  $B_t$ .

To prevent new tasks from interfering with past ones, O-LoRA requires the current task’s subspace  $\mathcal{U}_t$  to be orthogonal to all past task subspaces  $\mathcal{U}_i$  ( $i < t$ ). This orthogonality is enforced by constraining  $B_t$  such that:

$$O_{i,t} = B_i^\top B_t = \mathbf{0} \quad (3)$$

That is, the transpose of  $B_i$  (for  $i = 1, \dots, t-1$ ) multiplied by  $B_t$  yields a zero matrix, ensuring that the inner product of any vectors from the two subspaces is zero ( $\langle \mathbf{u}, \mathbf{w} \rangle = 0, \forall \mathbf{u} \in \mathcal{U}_i, \mathbf{w} \in \mathcal{U}_t$ ).

During training, an orthogonality loss term is added to the objective:

$$L_{\text{orth}}(B_i, B_t) = \sum_{j,k} |O_{i,t}[j, k]|^2$$

where  $O_{i,t}[j, k]$  denotes the element at the  $j$ -th row and  $k$ -th column of  $O_{i,t}$ . This reinforces the orthogonal constraint, minimizes inter-task interference, and mitigates catastrophic forgetting.

### 2.4 N-LoRA

In contrast to O-LoRA, N-LoRA (Yang et al., 2025) imposes a stronger constraint known as the non-parametric conflict condition.

**Definition 1** (Non-parametric Conflict). *For all  $(a, b)$ ,  $\Delta W_1[a, b] \cdot \Delta W_2[a, b] = 0$ , where  $\Delta W[a, b]$  denotes the element of  $\Delta W$  at row  $a$  and column  $b$ . If matrices  $\Delta W_1$  and  $\Delta W_2$  satisfy this condition,*

*they are said to be non-parametric conflicting at position  $(a, b)$ .*

Under this constraint, the previously updated parameter subspaces become more resistant to forgetting and sparser compared to O-LoRA, implying reduced parameter footprint and enabling more sequential adaptations. To reduce parameter collision, the authors apply  $\ell_1$  regularization to the LoRA parameters  $\Delta W_i$  of new tasks to enhance sparsity:

$$L_{\text{sparse}} = \lambda \|\Delta W_i\|_1 \quad (4)$$

### 2.5 LieRA

LieRA is a recently proposed parameter-efficient fine-tuning method. Unlike standard LoRA, (Si et al., 2025) treats parameters as elements of a Lie group and models updates as perturbations in the Lie algebra, preserving structure via the exponential map. Instead of the additive update  $W + \Delta W$  used in standard LoRA, LieRA employs a multiplicative update:

$$W \odot \exp(\Delta W), \quad (5)$$

where  $\exp(\Delta W)$  denotes the exponential mapping. This approach has demonstrated superior performance across various domains including computer vision (image classification, object detection/segmentation, image generation) and natural language processing (commonsense reasoning, language understanding). This fine-tuning method helps preserve the intrinsic structure of high-dimensional parameters (e.g., spatial locality in convolutional kernels), enhancing feature capture capability. The Lie group-Lie algebra framework ensures smooth and consistent updates, improving the model’s flexibility in adapting to new tasks. It retains the efficiency of low-rank adaptation while enhancing expressiveness through Hadamard product-based updates. Furthermore, it offers a geometric perspective on parameter updates.

## 3 Theoretical Framework

In this section, we introduce the theoretical framework of OLieRA, whose structure is illustrated in Figure 2. First, we adopt instruction tuning as the training paradigm. Second, we learn new tasks via incremental exponential maps under Hadamard product in orthogonal subspaces, while keeping the LoRA parameters of completed tasks fixed. In

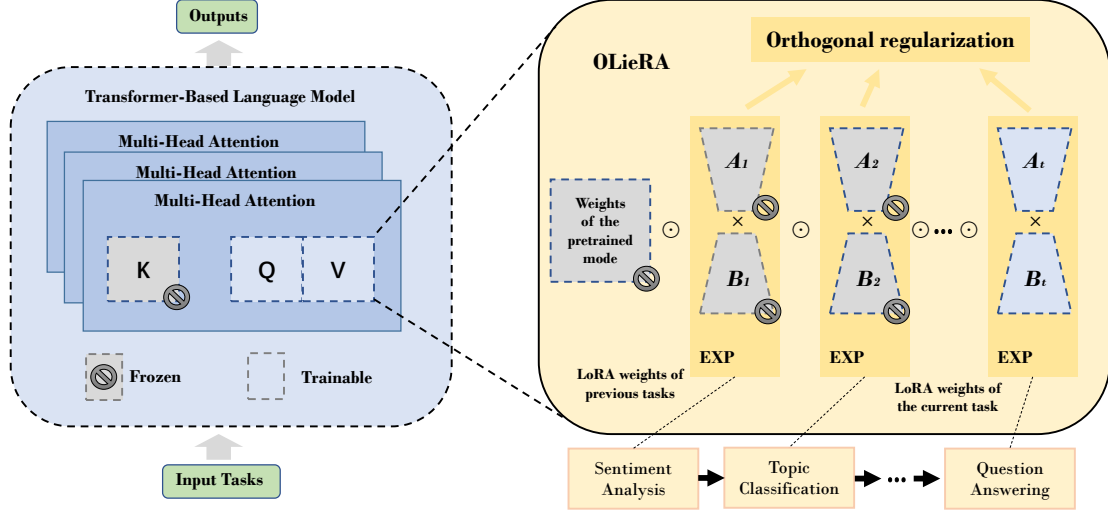


Figure 2: The OLieRA framework for continual learning in language models. First, human expertise is integrated and generalization is enhanced through instruction tuning. Second, building upon a frozen Transformer-based pre-trained language model, we leverage the exponential map of Lie groups to achieve "smooth manifold" parameter updates while preserving the intrinsic structure of the model. Then, we approximate the gradient subspace of each task using LoRA to efficiently control parameter overhead. For each sequentially arriving task, we incrementally learn a new LoRA module under both the Lie group constraint and an orthogonality constraint between the current task's LoRA subspace and all previous task subspaces, thereby reducing inter-task interference and preserving generalization to unseen tasks.

the next section, we provide a comparative analysis between the proposed method and existing approaches.

### 3.1 Introducing Lie Groups

To interpret parameter updates using Lie groups, we first need to construct a Lie group and attempt to describe the parameters within its framework. We consider collecting all possible instances of the parameters  $W$  into a set. It then suffices to define a well-defined operation on this set such that it satisfies the group structure, forms an Abelian group, and is a smooth manifold—thereby constituting a Lie group.

Define the set  $G = \{W \in \mathbb{R}^{b_1 \times b_2 \times \dots \times b_k} \mid W[a_1, a_2, \dots, a_k] \neq 0, \forall (a_1, a_2, \dots, a_k) \in ([1, b_1], [1, b_2], \dots, [1, b_k])\}$ . For practical reasons and operational convenience, we assume all elements are non-zero. A suitable approach is to use the Hadamard product  $\odot$  (element-wise multiplication) as the operation on this set. This is well-defined and causes all  $W$  to form a group, as it effectively reduces the operation to one-dimensional non-zero real multiplication, which itself is well-defined and forms a group. Furthermore, since multiplication on one-dimensional non-zero real numbers is commutative and a smooth manifold,

$(G, \odot)$  constitutes an Abelian group and a smooth manifold—i.e., a Lie group.

A rigorous verification is as follows. Note that:

- (1) The element  $I$  with all entries equal to 1 serves as the identity element.
- (2) Since every entry in any  $W$  is non-zero, the Hadamard product of any two  $W$  matrices also has all non-zero entries, satisfying closure.
- (3) Associativity follows from the associativity of one-dimensional real multiplication.
- (4) Commutativity follows from the commutativity of one-dimensional real multiplication.
- (5) Every element has an inverse (element-wise reciprocal), which exists due to the non-zero constraint.

Thus,  $(G, \odot)$  is an Abelian group.

### 3.2 Introducing Lie Algebras

If the Lie group  $(G, \odot)$  is viewed as a surface, then  $W$  belonging to this Lie group represents a point on that surface. The Lie algebra is the tangent plane at that point relative to the surface. Movement on the tangent plane is simpler because it is linear. Formally, the Lie algebra is a linear space. Treating  $W$  as a real vector, we can perform scalar multiplication and addition, forming a linear space denoted  $\mathfrak{g}$ .



Why introduce the Lie algebra? Because direct updates within the Lie group are cumbersome. Normally, to update, we would have:  $W_{\text{new}} = W_{\text{old}} \odot \Delta W$ , where  $W_{\text{new}}, W_{\text{old}}, \Delta W \in G$ . However, during optimization, we first compute the "required  $W_{\text{new}}$ " based on the loss function, and then invert to find the "amount to 'add'  $\Delta W$ ". This necessitates using the inverse element to solve for  $\Delta W$ : By "left-multiplying" both sides by the inverse of  $W_{\text{old}}$ , denoted  $W_{\text{old}}^{-1}$  (a property of groups: every element has an inverse satisfying  $W_{\text{old}} \odot W_{\text{old}}^{-1} = I$ ), we obtain:

$$\Delta W = W_{\text{old}}^{-1} \odot W_{\text{new}}$$

Therefore, it is preferable to first perform updates in the Lie algebra  $\mathfrak{g}$  and then map back to the Lie group via a specific mechanism. This returns us to the familiar tensor computations (addition and scalar multiplication) used in frameworks like PyTorch.

### 3.3 Improved Incremental Update Mechanism

For any  $W \in G$ , we do not directly modify  $W$  itself. Instead, we construct a small perturbation tensor  $\Delta W$  in the corresponding Lie algebra  $\mathfrak{g}$ .  $\Delta W$  is an ordinary tensor fully compatible with deep learning frameworks: gradients can be computed directly via `.grad`, linear updates can be performed using `.add_()` or `.mul_()`, and it can be adapted via reshape to existing fine-tuning methods designed for 2D tensors (e.g., LoRA), requiring no modifications to the optimization pipeline.

After performing the linear update on  $\Delta W$  in the Lie algebra  $\mathfrak{g}$ , it must be mapped "smoothly" back to the Lie group  $G$ . Directly updating via the Lie group multiplication  $W \odot \Delta W$  is problematic because  $\Delta W$  might not satisfy the constraints of  $G$  (e.g., all entries non-zero), potentially moving the result outside the valid parameter space. The exponential map  $\exp : \mathfrak{g} \rightarrow G$  is the crucial "bridge" connecting the Lie algebra to the Lie group. Its key roles are threefold:

1. **Local Homeomorphism:** For infinitesimal perturbations  $\Delta W$ ,  $\exp(\Delta W)$  maintains a local continuous correspondence with  $\Delta W$ , ensuring the result always lies within the valid parameter space of  $G$  and avoids parameter boundary issues (e.g., elements becoming zero);

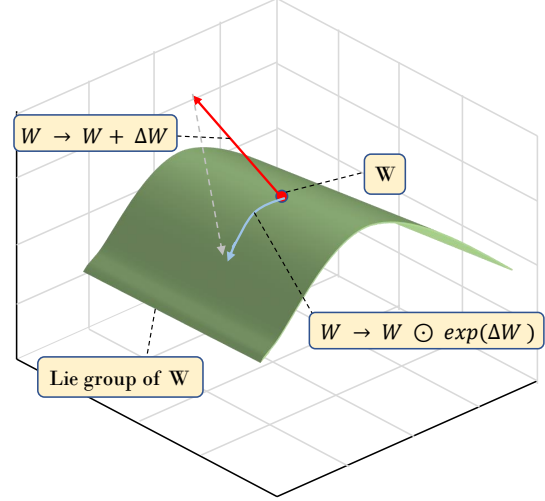


Figure 3: Illustration of the difference between the improved incremental update mechanism and the previous approach.

2. **Structure Preservation:** The result of  $\exp(\Delta W)$  necessarily belongs to  $G$ , and the mapping is implemented via element-wise exponential scaling—only adjusting the numerical proportions of the weights without disrupting the tensor dimensions or topological structure of the parameter space;
3. **Geometric Consistency:** It guides weight updates along the natural gradient direction of the Lie group manifold, avoiding the issue of "update direction decoupling from manifold geometry" inherent in ordinary linear addition (e.g.,  $W_{\text{new}} = W_{\text{old}} + \Delta W$ ).

Based on this, the weight update formula can be expressed as:

$$W \mapsto W \odot \exp(\Delta W) \quad (6)$$

This formulation ensures the legality of the group operation via the Lie group multiplication  $\odot$  (Hadamard product), while leveraging the linear properties of the Lie algebra to simplify the optimization of  $\Delta W$ , achieving a balance between "structural constraints" and "optimization efficiency". Figure 3 visually illustrates the difference before and after this improvement.

### 3.4 First-Order Taylor Approximation of the Exponential Map

Since  $\Delta W$  is small, the exponential map can be approximated using its first-order Taylor expansion:

$$\exp(\Delta W) = I + \Delta W + o(\|\Delta W\|) \quad (7)$$

where  $I$  denotes the matrix of all ones, and  $o(\|\Delta W\|)$  represents a remainder term. As  $\|\Delta W\|$  approaches zero, this remainder becomes negligible compared to  $\|\Delta W\|$  in an asymptotic sense. Therefore, we approximate the exponential map as  $\exp(\Delta W) \approx I + \Delta W$ . Substituting this approximation into the multiplicative update yields:

$$W \odot \exp(\Delta W) \approx W \odot (I + \Delta W) = W + W \odot \Delta W \quad (8)$$

### 3.5 Higher-Order Taylor Approximation of the Exponential Map

For greater accuracy, we can employ a higher-order Taylor expansion of the exponential map:

$$\exp(\Delta W) = I + \Delta W + \frac{1}{2} \Delta W \odot \Delta W + o(\|\Delta W \odot \Delta W\|) \quad (9)$$

This is the second-order expansion. Essentially, this involves performing a higher-order Taylor expansion on each element individually.

### 3.6 Low-Rank Decomposition

We apply low-rank decomposition to  $\Delta W$ :

$$\Delta W = BA \quad (10)$$

where  $B \in \mathbb{R}^{\text{out} \times r}$ ,  $A \in \mathbb{R}^{r \times \text{in}}$ , and  $r \ll \min(\text{out}, \text{in})$ .

Substituting into the multiplicative update, we get:

$$\begin{aligned} W \odot \exp(\Delta W) &\approx W \odot (I + \Delta W) \\ &= W + W \odot \Delta W \\ &= W + W \odot (BA) \end{aligned} \quad (11)$$

Note: Matrix multiplication has higher precedence than the Hadamard product.

### 3.7 Orthogonality Loss Calculation

To mitigate catastrophic forgetting, we constrain the parameter space of each update to be as orthogonal as possible to the parameter spaces of all previous updates. Importantly, unlike (Wang et al., 2023a), our method applies the orthogonality constraint not just to the matrices  $B$ , but to the entire final updated parameter space, i.e., to  $\exp(\Delta W)$ .

Thus, we add a new loss term as follows:

$$\begin{aligned} \mathcal{L}_{\text{orth}} &= \sum_{i \neq j} \left\| \exp(\Delta W_i) \exp(\Delta W_j)^\top \right\|_F \\ &\approx \sum_{i \neq j} \left\| (I + B_i A_i)(I + B_j A_j)^\top \right\|_F \end{aligned} \quad (12)$$

where:

- $\|\cdot\|_F$  denotes the Frobenius norm (i.e.,  $\sqrt{\sum_{k,l} |M_{kl}|^2}$ )
- The summation is over all pairs of previous tasks for the model.

## 3.8 Complete Formulation

After incorporating the orthogonality constraint, the final total loss function is:

$$\mathcal{L}_{\text{total}} = \mathcal{L}_{\text{task}} + \lambda \sum_{i \neq j} \left\| (I + B_i A_i)(I + B_j A_j)^\top \right\|_F \quad (13)$$

where  $\lambda$  controls the strength of the orthogonality penalty term.

## 4 Experimental Results

### 4.1 Experimental Setup

#### Datasets.

To evaluate the effectiveness of our method, we follow O-LoRA (Wang et al., 2023a) and N-LoRA (Yang et al., 2025) and utilize two benchmark datasets: 1) the Standard CL Benchmark, which comprises 5 text classification datasets, and 2) the Multi-Task Benchmark, which consists of 15 datasets, including those from GLUE, SuperGLUE, and IMDB. We adhere to the experimental protocols established by LFPT5 (Qin and Joty, 2021), O-LoRA (Wang et al., 2023a), and N-LoRA (Yang et al., 2025), employing three different task sequences for each benchmark dataset. Further details are provided in the Appendix.

#### Metrics.

Let  $a_{i,j}$  denote the test accuracy on the  $i$ -th task after training on the  $j$ -th task. The evaluation metric adopted in this study is:

**Average Accuracy (AA)**, defined as the mean accuracy across all tasks after training on the final task is completed. It is calculated as  $A_T = \frac{1}{T} \sum_{i=1}^T a_{i,T}$ , where  $T$  is the total number of tasks.

#### Baseline Methods.

To validate the effectiveness of OLieRA, we compare, as in O-LoRA (Wang et al., 2023a) and N-LoRA (Yang et al., 2025), against the following baseline methods:

#### i. Isolated Training Methods

- *PerTaskFT*: Trains an independent model for each task.
- *Prog-Prompt* (Razdaibiedina et al., 2023): Learns isolated prompts for each

task, essentially equivalent to training a distinct model per task.

## ii. Upper Bound Method

- *Multi-Task Learning (MTL)*: Trains a single model on all tasks simultaneously. This method serves as the performance upper bound for continual learning.

## iii. Non-Continual Learning Methods

- *SeqFT* (de Masson d’Autume et al., 2019): Finetunes all model parameters sequentially across the task sequence.
- *SeqLoRA*: Trains a single LoRA adapter across the task sequence while keeping the pre-trained model parameters frozen.
- *IncLoRA*: Trains a new LoRA module for each task.

## iv. Continual Learning Methods

- *Replay*: Replays samples from previous tasks via a memory buffer while finetuning all model parameters.
- *EWC* (Kirkpatrick et al., 2017): Applies a Fisher regularization loss to adjust all model parameters.
- *LwF* (Li and Hoiem, 2018): Preserves knowledge from previous tasks by recording the outputs of the previous task’s model on new task data and using these outputs as a regularization term.
- *L2P* (Wang et al., 2021) and *LFPT5* (Qin and Joty, 2021): Both employ prompt-based mechanisms, adapting to new tasks by dynamically selecting or generating prompts.
- *O-LoRA* (Wang et al., 2023a): Incrementally updates parameters for new tasks by constraining them to lie in the orthogonal subspace of parameters from previous tasks, while keeping the LoRA parameters learned from previous tasks fixed.
- *N-LoRA* (Yang et al., 2025): Learns parameters for new tasks in a non-parametric conflicting space under a stronger constraint than orthogonality (non-parametric conflict condition), while fixing the LoRA parameters learned previously, enabling incremental updates for new tasks.

## 4.2 Comparison with State-of-the-Art Methods

Tables 1 and 2 present the performance comparison, measured by Average Accuracy ( $A_T$ ), between OLieRA and other baseline methods across different benchmark datasets. Following the experimental setup of LFPT5 (Qin and Joty, 2021), O-LoRA (Wang et al., 2023a), and N-LoRA (Yang et al., 2025), we report the results from three independent runs with different task sequences and models on the Continual Learning (CL) benchmark dataset.

### Performance on the Standard Continual Learning Benchmark.

OLieRA demonstrates stable and outstanding performance across the three task sequences (Order-1, Order-2, Order-3) of this benchmark: it achieves scores of 79.9, 79.5, and 79.5, respectively, with an average performance (avg) of 79.6. This notably:

- Surpasses the previous state-of-the-art (SOTA) method N-LoRA by 0.8% (compared to N-LoRA’s avg of 78.8).
- Outperforms isolated training methods such as ProgPrompt (avg 75.1) and PerTaskFT (avg 70.0).
- Performs exceedingly close to the continual learning upper bound—MTL (avg 80.0)—with a mere gap of 0.4%, indicating that OLieRA can utilize knowledge from multiple tasks with high efficiency.

As shown in Table 2, OLieRA also significantly outperforms O-LoRA and mostly slightly surpasses N-LoRA on the larger-scale LLaMA-7B model. This validates that our proposed method remains effective even on larger-scale Large Language Models (LLMs).

### Performance in the Multi-Task Scenario.

Continual learning involving a large number of tasks constitutes a significantly more challenging benchmark scenario. As shown in Table 1, under task sequences 4, 5, and 6, OLieRA’s performance exceeds that of all existing state-of-the-art methods, achieving an average performance gain of 0.2%. These results robustly demonstrate that OLieRA excels at preserving task-specific knowledge while handling a large number of tasks, exhibiting superior overall performance.

Benchmarks Methods	Standard CL Benchmark				Large Number of Tasks			
	Order-1	Order-2	Order-3	avg	Order-4	Order-5	Order-6	avg
ProgPrompt	75.2	75.0	75.1	75.1	78.0	77.7	77.9	77.9
PerTaskFT	70.0	70.0	70.0	70.0	78.1	78.1	78.1	78.1
MTL	80.0	80.0	80.0	80.0	76.5	76.5	76.5	76.5
SeqFT	18.9	24.9	41.7	28.5	7.4	7.4	7.5	7.4
SeqLoRA	44.6	32.7	53.7	43.7	0.6	1.9	1.6	1.6
IncLoRA	66.0	64.9	68.3	66.4	63.3	58.5	61.7	61.2
Replay	55.2	56.9	61.3	57.8	55.0	54.6	53.1	54.2
EWC	48.7	47.7	54.5	50.3	45.3	44.5	45.6	45.1
LwF	54.4	53.1	49.6	52.3	50.1	43.1	47.4	46.9
L2P	60.3	61.7	61.1	60.7	57.5	53.8	56.9	56.1
LFPT5	67.6	72.6	77.9	72.7	70.4	68.2	69.1	69.2
O-LoRA	75.4	75.7	76.3	75.8	72.3	64.8	71.6	69.6
N-LoRA	79.2	78.4	78.8	78.8	73.6	70.3	73.2	72.4
<b>OLieRA</b>	<b>79.9</b>	<b>79.5</b>	<b>79.5</b>	<b>79.6</b>	<b>73.8</b>	<b>70.4</b>	<b>73.5</b>	<b>72.6</b>

Table 1: Summary of results on two standard continual learning benchmarks using the T5-large model. The average accuracy after training on the final task is reported, with all results averaged over three independent runs.

Benchmarks	Order-1	Order-2	Order-3	avg
O-LoRA	76.8	75.7	75.7	76.1
N-LoRA	77.2	77.3	<b>78.4</b>	77.6
OLieRA	<b>77.4</b>	<b>77.5</b>	78.3	<b>77.7</b>

Table 2: Performance comparison between N-LoRA, O-LoRA and OLieRA on the larger LLaMA-7B model, reporting average accuracy across all task orders. Results are averaged over three independent runs.

## 5 Discussion

### 5.1 Interpretation via Lie Group Introduction

Inspired by (Si et al., 2025), we can interpret the pre-trained parameters  $W$  as elements of a Lie group. The fine-tuning adjustment  $\Delta W$  applied to these parameters can then be viewed as an infinitesimal perturbation of this element. The elements of the corresponding Lie algebra constitute a specific collection of such infinitesimal perturbations (i.e., perturbations on the tangent plane). Crucially, infinitesimal perturbations from the Lie algebra can be mapped back to the Lie group via structure-preserving maps, such as the exponential map, ensuring the perturbed element remains within the group. This is the fundamental rationale behind Lie algebras: direct additive changes to Lie group elements do not guarantee the result stays within the group. The Lie algebra formalism, coupled with a structure-preserving mapping like the exponential map, allows us to constrain the parameter update  $\Delta W$  to be a valid infinitesimal perturbation (satisfying Lie algebra conditions), thereby achieving the desired effect of preserving the Lie group structure.

A prerequisite for this approach is that  $W$  itself possesses a structure worth preserving. (Si et al., 2025) demonstrated that convolutional kernels indeed benefit from such structure-preserving constraints during fine-tuning. We posit that Large Language Models (LLMs) also contain structures that need preservation. While the structure in LLMs differs from the spatial locality crucial for convolutional kernels and is more challenging to interpret directly due to the model’s complexity, some explanations can be offered.

LLMs comprise diverse layers, such as the Q/K/V matrices in Transformer layers, Feed-Forward network weights, layer normalization parameters, etc. **First**, these modules exhibit internal structures, much like trained convolutional kernels. Certain aspects of these structures must be preserved, as even minor alterations could catastrophically disrupt performance on previously learned tasks—the essence of catastrophic forgetting. **Second**, these modules are not isolated; they are intricately interconnected with complex, abstract relationships. Preserving these inter-modular relationships is another crucial aspect of the overall structure.

Based on this reasoning, we argue that employing Lie group and Lie algebra theory for parameter updates to preserve structure is necessary. Consequently, we use  $W \odot \exp(\Delta W)$  for parameter updates instead of  $W + \Delta W$ . Furthermore, we can still apply low-rank decomposition to  $\Delta W$  within  $\exp(\Delta W)$ , thus retaining the advantages associated with low-rank adaptation.



## 5.2 Order of Taylor Expansion

In practice, to reduce computational overhead, we can approximate the exponential map using its Taylor expansion. While the resulting perturbation is not perfectly structure-preserving, it offers a close approximation. By expanding to a higher order, we can achieve a better fit to the ideal structure-preserving perturbation, analogous to approximating a continuous curve with a polynomial function. Consequently, we posit that the order of the Taylor expansion influences the final structure-preserving effect—higher orders yield approximations that more closely resemble the ideal infinitesimal perturbation that perfectly preserves structure. The mathematical expression for the  $n$ -th order Taylor expansion of the exponential map is as follows:

$$\exp(\Delta W) = I + \Delta W + \frac{1}{2!}\Delta W^{\odot 2} + \dots + \frac{1}{n!}\Delta W^{\odot n} + o(\|\Delta W^{\odot n}\|) \quad (14)$$

where  $I$  denotes the matrix of all ones, and  $\Delta W^{\odot 2}$  represents the Hadamard (element-wise) product  $\Delta W \odot \Delta W$ .

To investigate this, we conducted an ablation study: on the Standard CL Benchmark, using the T5 base model, we trained models utilizing first-order, second-order, and third-order Taylor approximations, respectively. The final results, reported as the average over three independent runs, are presented in Table 3.

Taylor order	1st-order	2nd-order	3rd-order
Order-1	79.4	79.9	79.9
Order-2	79.2	79.5	79.6
Order-3	79.3	79.5	79.4

Table 3: The performance of model on Standard CL Benchmark using the T5-large model with first-order, second-order and third-order Taylor approximation. Results are averaged over three independent runs.

## 5.3 Effectiveness of the Multiplicative Update

To validate the necessity of the multiplicative update from the Lie group perspective, we conducted a critical ablation study. Under the condition of keeping the full subspace orthogonality constraint loss function unchanged, we replaced the proposed multiplicative parameter update ( $W \odot \exp(\Delta W)$ ) with the standard additive update ( $W + \Delta W$ ). This

ablated model is denoted as "No LieGroup Mult". The experimental results are presented in Table 4.

A significant and consistent performance degradation (an average drop of approximately 2.3%) is observed across all task sequences of the Standard CL Benchmark when the multiplicative update mechanism is removed. This result strongly demonstrates that the exponential map-based multiplicative update adopted in this work is crucial for achieving optimal performance. It is not merely a replaceable implementation detail but a core component of the OLieRA method, working synergistically with the orthogonality constraint.

We hypothesize that the multiplicative update, due to its scaling nature, better preserves the intrinsic structure of the pre-trained weights. This provides a more stable and accommodating parameter space foundation for the subsequent orthogonally constrained updates for new tasks. Without this geometric structure-preserving mechanism, the effectiveness of the subspace orthogonality constraint is substantially diminished.

Fisher value	Order-1	Order-2	Order-3
OLieRA	79.9	79.5	79.5
No LieGroup Mult	77.4	77.2	76.9

Table 4: The ablation experiment of effectiveness of multiplicative updates on Standard CL Benchmark using the T5-large model. Results are averaged over three independent runs.

## 5.4 Unveiling the Internal Mechanism via Fisher Information

In continual learning, the Fisher Information Matrix is commonly used to quantify the importance of parameters for previously learned tasks. Given model parameters  $\theta$ , the  $i$ -th diagonal element of the Fisher Information Matrix is typically approximated empirically as:

$$F_i \approx \mathbb{E}_{x \sim \mathcal{D}} \left[ \left( \frac{\partial}{\partial \theta_i} \log p(y|x; \theta) \right)^2 \right], \quad (15)$$

where  $\mathcal{D}$  is the data distribution of the old task and  $\theta_i$  denotes the  $i$ -th parameter of the model. A larger  $F_i$  indicates that the corresponding parameter direction is more sensitive to the performance of the old tasks, and thus should be more strongly protected during subsequent fine-tuning.

In LoRA-based continual learning methods, the learning process for each task introduces a parameter increment  $\Delta\theta$ . To quantify the degree of conflict

between the updates for new and old tasks, we can define a Fisher-weighted energy metric for  $\Delta\theta$  under the diagonal Fisher approximation (Kirkpatrick et al., 2017):

$$E = \sum_i F_i(\Delta\theta_i)^2. \quad (16)$$

This metric describes the "energy" of the new task's update within the sensitive directions of the old tasks. Intuitively, a larger  $E$  indicates that the parameter update for the new task causes stronger perturbations along directions important to the old tasks, posing a higher risk of catastrophic forgetting. Conversely, a smaller  $E$  suggests that the new task's update is more concentrated in directions with lower Fisher information, thereby having a relatively limited impact on the old tasks.

Fisher value	Order-1	Order-2	Order-3
O-LoRA	0.12	0.09	0.42
N-LoRA	7e-11	8e-11	1e-10
OLieRA	1.04	1.43	3.92

Table 5: The Fisher value of model on Standard CL Benchmark using the T5-large model with different methods. Results are averaged over three independent runs.

We computed the Fisher-weighted energy of  $\Delta\theta$  between the last and the penultimate tasks. The results are presented in Table 5. As shown, the Fisher Energy value of N-LoRA is close to zero, with a magnitude significantly smaller than that of O-LoRA, which is consistent with the observation in (Yang et al., 2025) that N-LoRA achieves stronger orthogonality. Interestingly, in our experiments we found that OLieRA exhibits the opposite trend: its Fisher-weighted  $\Delta\theta$  energy is higher than that of the other two baseline methods. This result suggests that, by employing exponential mapping and enforcing orthogonality in the Lie group parameter space, OLieRA does not merely avoid updates along the sensitive directions of previous tasks. Instead, it allows updates even in directions with large Fisher values. We argue that this strategy enhances parameter utilization, enabling new tasks to better leverage the important representations already learned. As a result, OLieRA achieves stronger expressiveness and superior overall performance, striking a balance between mitigating task interference and promoting knowledge sharing.

## 6 Conclusion

Through both theoretical derivation and empirical validation, this work demonstrates that enforcing orthogonality constraints on the full task-update subspace—while preserving the inherent structure of pretrained model parameters—is a key strategy for mitigating catastrophic forgetting in large language models (LLMs). Building on this insight, we propose **OLieRA** (Orthogonal Low-rank adaptation in Lie groups), a method that combines theoretical interpretability with practical efficiency. By integrating a multiplicative update paradigm grounded in Lie group theory (which preserves the geometric structure of parameters), full-subspace orthogonality constraints (which reduce task interference), and Taylor approximation techniques (which balance accuracy and computational cost), OLieRA achieves a new breakthrough in continual learning performance.

Comprehensive experiments on both the standard CL benchmark (5 text classification tasks) and the long-sequence multi-task benchmark (15 tasks spanning GLUE and SuperGLUE) demonstrate that, compared with state-of-the-art methods such as O-LoRA and N-LoRA, OLieRA not only maintains parameter structure while enforcing full-subspace orthogonality, but also delivers superior average accuracy (79.6% on the standard CL benchmark, approaching the MTL upper bound; 72.6% on the multi-task benchmark, surpassing existing methods). Moreover, OLieRA provides stronger resistance to task interference while retaining the key advantages of O-LoRA—no need for historical data storage (privacy-friendly), only a small number of additional parameters (cost-efficient), and independence from task IDs at test time (compatible with instruction-tuning generalization). Finally, Fisher information analysis further confirms that OLieRA enables controlled updates along sensitive parameter directions of prior tasks, effectively balancing task conflict with knowledge sharing, and offering a novel paradigm toward practical continual learning for LLMs.

## References

- Cyprien de Masson d’Autume, Sebastian Ruder, Lingpeng Kong, and Dani Yogatama. 2019. Episodic memory in lifelong language learning. *CoRR*, abs/1906.01076.
- Edward J. Hu, Yelong Shen, Phillip Wallis, Zeyuan Allen-Zhu, Yuanzhi Li, Shean Wang, Lu Wang, and

- Weizhu Chen. 2021. Lora: Low-rank adaptation of large language models.
- Zixuan Ke and Bing Liu. 2023. Continual learning of natural language processing tasks: A survey.
- James Kirkpatrick, Razvan Pascanu, Neil Rabinowitz, Joel Veness, Guillaume Desjardins, Andrei A Rusu, Kieran Milan, John Quan, Tiago Ramalho, Agnieszka Grabska-Barwinska, and 1 others. 2017. Overcoming catastrophic forgetting in neural networks. *Proceedings of the national academy of sciences*, 114(13):3521–3526.
- Zhizhong Li and Derek Hoiem. 2018. Learning without forgetting. *IEEE Transactions on Pattern Analysis and Machine Intelligence*, 40(12):2935–2947.
- Michael McCloskey and Neal J. Cohen. 1989. Catastrophic interference in connectionist networks: The sequential learning problem. volume 24 of *Psychology of Learning and Motivation*, pages 109–165. Academic Press.
- Chengwei Qin and Shafiq R. Joty. 2021. LFPT5: A unified framework for lifelong few-shot language learning based on prompt tuning of T5. *CoRR*, abs/2110.07298.
- Anastasia Razdaibiedina, Yuning Mao, Rui Hou, Madihan Khabza, Mike Lewis, and Amjad Almahairi. 2023. Progressive prompts: Continual learning for language models. In *The Eleventh International Conference on Learning Representations*.
- Chongjie Si, Zhiyi Shi, Xuehui Wang, Yichen Xiao, Xiaokang Yang, and Wei Shen. 2025. Generalized tensor-based parameter-efficient fine-tuning via lie group transformations. In *arXiv preprint arXiv:2504.00851v2*.
- Alex Wang, Yada Pruksachatkun, Nikita Nangia, Amanpreet Singh, Julian Michael, Felix Hill, Omer Levy, and Samuel Bowman. 2019. Superglue: A stickier benchmark for general-purpose language understanding systems. *Advances in neural information processing systems*, 32.
- Alex Wang, Amanpreet Singh, Julian Michael, Felix Hill, Omer Levy, and Samuel R Bowman. 2018. Glue: A multi-task benchmark and analysis platform for natural language understanding. *arXiv preprint arXiv:1804.07461*.
- Xiao Wang, Tianze Chen, Qiming Ge, Han Xia, Rong Bao, Rui Zheng, Qi Zhang, Tao Gui, and Xuanjing Huang. 2023a. Orthogonal subspace learning for language model continual learning. In *Findings of the Association for Computational Linguistics: EMNLP 2023*, pages 10658–10671.
- Xiao Wang, Yuansen Zhang, Tianze Chen, Songyang Gao, Senjie Jin, Xianjun Yang, Zhiheng Xi, Rui Zheng, Yicheng Zou, Tao Gui, Qi Zhang, and Xuanjing Huang. 2023b. Trace: A comprehensive benchmark for continual learning in large language models.
- Zifeng Wang, Zizhao Zhang, Chen-Yu Lee, Han Zhang, Ruoxi Sun, Xiaoqi Ren, Guolong Su, Vincent Perot, Jennifer G. Dy, and Tomas Pfister. 2021. Learning to prompt for continual learning. *Computing Research Repository*, abs/2112.08654.
- Shuo Yang, Kun-Peng Ning, Yu-Yang Liu, Jia-Yu Yao, Yong-Hong Tian, Yi-Bing Song, and Li Yuan. 2025. Is parameter collision hindering continual learning in LLMs? In *Proceedings of the 31st International Conference on Computational Linguistics*, pages 4243–4259.
- Xiang Zhang, Junbo Zhao, and Yann LeCun. 2015. Character-level convolutional networks for text classification. *Advances in neural information processing systems*, 28.

## A Appendix

### A.1 Experimental Details

All experiments with the T5 model were conducted on a single machine equipped with an NVIDIA A100-SXM4-80GB GPU, and implemented based on the DeepSpeed library. For all task order sequences, we trained the models with the following unified hyperparameters: the number of training epochs was set to 2, the learning rate was fixed at  $1e-3$  for the Standard CL Benchmark and  $5e-4$  for the Large Number of Tasks setting, the dropout rate was set to 0.1, and the weight decay rate was set to 0. The only exceptions occur in Orders 1–6, where the values of  $\lambda_1$  and  $\lambda_2$  differ as follows:

For Order-1, Order-2, and Order-3, we set  $\lambda_1 = 0.5$  and  $\lambda_2 = 0$ . For Order-4 (with the task sequence MNLI, CB, WiC, COPA, QQP, BoolQA, RTE, IMDB, Yelp, Amazon, SST-2, DBpedia, Agnews, MultiRC, Yahoo), the values of  $\lambda_1$  were set to 0.5, 0.5, 0.5, 0.5, 0.5, 0.5, 0.5, 0.5, 0.5, 0.5, 0.5, 0.6, 0.7, 0.4, 0.6, and  $\lambda_2$  to 0, 0, 0.1, 0, 0, 0, 0, 0, 0, 0, 0.01, 0.02, 0, 0.05. For Order-5 (with the task sequence MultiRC, BoolQA, WiC, MNLI, CB, COPA, QQP, RTE, IMDB, SST-2, DBpedia, Agnews, Yelp, Amazon, Yahoo), the values of  $\lambda_1$  were set to 0.7, 0.7, 0.7, 0.7, 0.7, 0.7, 0.7, 0.7, 0.7, 0.7, 0.7, 0.7, 0.5, 0.7, 0.4, 1, and  $\lambda_2$  to 0, 0, 0, 0, 0, 0, 0, 0, 0, 0, 0.05, 0.04, 0.08, 0.15. For Order-6 (with the task sequence Yelp, Amazon, MNLI, CB, COPA, QQP, RTE, IMDB, SST-2, DBpedia, Agnews, Yahoo, MultiRC, BoolQA, WiC),  $\lambda_1$  was uniformly set to 1.1 and  $\lambda_2$  to 0.

For experiments with the LLAMA-7B model, we adopted the following settings: For all orders,  $\lambda_1$  was set to 0.5 and  $\lambda_2$  to 0. For tasks in Order-1, the learning rates were set to ( $1e-3$ ,  $1e-4$ ,  $1e-4$ ,  $1e-4$ ), batch sizes to (8, 4, 8, 8), dropout rate to

0.1, weight decay to 0, and the number of training epochs to (1, 2, 1, 2). For tasks in Order-2, the learning rates were set to (1e-3, 1e-4, 1e-4, 1e-4), batch sizes to (8, 4, 8, 8), dropout rate to 0.1, weight decay to 0, and the number of training epochs to (1, 2, 2, 1). For tasks in Order-3, the learning rates were set to (1e-3, 1e-4, 1e-4, 1e-4), batch sizes to (8, 4, 8, 8), dropout rate to 0.1, weight decay to 0, and the number of training epochs to (1, 2, 2, 1).

## A.2 Datasets

Table 6 provides detailed descriptions of the 15 datasets and their evaluation metrics used in our continual learning (CL) experiments. Overall, the datasets were drawn from three main benchmark suites: the CL benchmark (Zhang et al., 2015), GLUE (Wang et al., 2018), and SuperGLUE (Wang et al., 2019). In addition, following (Razdaibiedina et al., 2023), we supplemented these benchmarks with the IMDB movie reviews dataset.

## A.3 Task Sequence Orders

We report the task sequences used in our CL experiments in Table 7.

## A.4 Task Instructions

Table 8 presents the prompts used for different tasks. NLI denotes Natural Language Inference, including MNLI, RTE, and CB. SC denotes Sentiment Classification, including Amazon, Yelp, SST-2, and IMDB. TC denotes Topic Classification, including AGNews, Dbpedia, and Yahoo.

Dataset name	Category	Task	Domain	Metric
1. Yelp	CL Benchmark	sentiment analysis	Yelp reviews	accuracy
2. Amazon	CL Benchmark	sentiment analysis	Amazon reviews	accuracy
3. DBpedia	CL Benchmark	topic classification	Wikipedia	accuracy
4. Yahoo	CL Benchmark	topic classification	Yahoo Q&A	accuracy
5. AG News	CL Benchmark	topic classification	news	accuracy
6. MNLI	GLUE	NLI	various	accuracy
7. QQP	GLUE	paragraph detection	Quora	accuracy
8. RTE	GLUE	NLI	news, Wikipedia	accuracy
9. SST-2	GLUE	sentiment analysis	movie reviews	accuracy
10. WiC	SuperGLUE	word sense disambiguation	lexical databases	accuracy
11. CB	SuperGLUE	NLI	various	accuracy
12. COPA	SuperGLUE	QA	blogs, encyclopedia	accuracy
13. BoolQA	SuperGLUE	boolean QA	Wikipedia	accuracy
14. MultiRC	SuperGLUE	QA	various	accuracy
15. IMDB	SuperGLUE	sentiment analysis	movie reviews	accuracy

Table 6: The details of 15 datasets used in our CL experiments. NLI denotes natural language inference, QA denotes questions and answers task. First five tasks correspond to the standard CL benchmark, all other tasks are used in long-sequence experiments.

Order	Model	Task Sequence
1	T5, LLaMA	dbpedia → amazon → yahoo → ag
2	T5, LLaMA	dbpedia → amazon → ag → yahoo
3	T5, LLaMA	yahoo → amazon → ag → dbpedia
4	T5	mnli → cb → wic → copa → qqp → boolqa → rte → imdb → yelp → amazon → sst-2 → dbpedia → ag → multirc → yahoo
5	T5	multirc → boolqa → wic → mnli → cb → copa → qqp → rte → imdb → sst-2 → dbpedia → ag → yelp → amazon → yahoo
6	T5	yelp → amazon → mnli → cb → copa → qqp → rte → imdb → sst-2 → dbpedia → ag → yahoo → multirc → boolqa → wic

Table 7: Six different orders of task sequences used for continual learning experiments. Orders 1-3 correspond to the standard CL benchmark adopted by prior works. Orders 4-6 are long-sequence orders spanning 15 tasks, following (Razdaibiedina et al., 2023).

Task	Prompts
NLI	What is the logical relationship between the "sentence 1" and the "sentence 2"? Choose one from the option.
QQP	Whether the "first sentence" and the "second sentence" have the same meaning? Choose one from the option.
SC	What is the sentiment of the following paragraph? Choose one from the option.
TC	What is the topic of the following paragraph? Choose one from the option.
BoolQA	According to the following passage, is the question true or false? Choose one from the option.
MultiRC	According to the following passage and question, is the candidate answer true or false? Choose one from the option.
WiC	Given a word and two sentences, whether the word is used with the same sense in both sentence? Choose one from the option.

Table 8: Instructions for different tasks.